Postextrusion Heating in Three-Dimensional Printing

David A. Edwards[1]
Department of Mathematical Sciences,
University of Delaware,
Newark, DE 19716
e-mail: dedwards@udel.edu

Michael E. Mackay
Department of Materials Science
and Engineering,
University of Delaware,
Newark, DE 19716

Stresses result when polymer feed stock is extruded through the nozzle of a three-dimensional (3D) printer, causing undesirable surface roughness called "sharkskin," which hinders effective bonding to the substrate. A promising method to remove the sharkskin is to reheat the polymer after extrusion. However, questions remain about the appropriate design parameters to guarantee success. A mathematical model is presented for this system, and both amorphous and crystalline polymers are examined. The former is a heat transfer problem; the latter a Stefan problem. Several effectiveness conditions are considered, including exit temperature and a duration condition related to the polymer relaxation time. Our results provide guidance on designing effective postextrusion heaters. [DOI: 10.1115/1.4046343]

Keywords: 3D printing, additive manufacturing, sharkskin, heat transfer, asymptotics, Stefan problem

1 Introduction

With improvements in technology and reductions in cost, three-dimensional (3D) printing (or additive manufacturing) has become incredibly popular. It is used in wide ranges of applications, from industrial production of prototypes to consumer production of various devices and gadgets [1]. Especially, in the industrial setting, it is desirable to manufacture as quickly as possible. However, doing so can lead to defects in the extruded material that inhibit effective bonding to the substrate.

In a 3D printer, a flexible polymer thread is extruded from a "hot end" at velocity V. Within the hot end, the polymer can be thought of as a fluid subject to the no-slip condition at the wall. However, after extrusion the thread moves according to plug flow. The resultant rapid acceleration of the polymer surface causes a stress singularity at the exit of the hot end [2]. These stresses cause periodic irregularities (commonly called "sharkskin") to form on the outer surface of the polymer thread [2–4]. These irregularities can inhibit bonding to the substrate.

One innovative idea to remove these defects is to reheat the extruded thread by running it through a "washer heater" (so-called because a prototype is an ordinary metal washer). The thread then exits into the open air before being deposited onto the existing 3D printout substrate. Engineers would like to design the washer heater as efficiently as possible with two goals in mind:

(1) Heat the outer surface of the polymer to a temperature $\tilde{T}_r$ (the "r" denotes "relaxation") for long enough that the viscoelastic polymer relaxes, removing the sharkskin roughness.
(2) Heat the outer surface of the polymer enough so it is significantly warmer at deposition, further enhancing bonding. (For more discussion of the negative effects of heat loss before deposition, see Ref. [5].)

The experimental parameters at our disposal for the washer heater are its height $\tilde{H}_w$ and temperature $\tilde{T}_w$, where the subscript "w" refers to "washer." Hence, we wish to know, for a given $\tilde{H}_w$, what is the minimum $\tilde{T}_w$ needed to remove the sharkskin, or vice versa.

We model the system as a heat transfer problem in cylindrical coordinates in Sec. 2. There are two main types of polymers used in 3D printing: amorphous polymers such as acrylonitrile butadiene styrene (ABS), and crystalline polymers such as polylactic acid (PLA) [6,7]. In the amorphous case treated in Sec. 3, the rigid and pliant regions have similar material properties, and the problem has an analytically tractable solution. However, it is not obvious which constraint on the mathematical system translates into results which match the experimental data. In Sec. 4, we consider two possibilities: the exit temperature and a duration above a threshold temperature.

As shown in Sec. 5, a formal treatment of the crystalline case involves a Stefan-like problem. Introducing the quasi-stationary approximation yields analytically tractable solutions. Only the minimum duration condition requires the use of the crystalline approximation.

Our results demonstrate that goal #2 above is unrealistic, as the polymer thread cools quite rapidly when exposed to the air, no matter the exit temperature. As for goal #1, it is possible to relax the sharkskin at experimentally realizable temperatures for reasonably thick washers. Either the exit or duration condition provides a computable threshold, though the duration condition has the advantage of an interpretation in terms of the polymer relaxation time. The additional complication of introducing the Stefan problem for the crystalline case is demonstrated to affect the results only slightly. Hence, as in Ref. [8], treating any crystalline polymer as amorphous will not significantly degrade the model's performance.

2 Governing Equations

We model the system as shown in Fig. 1. We consider heat transfer of a polymer passing through a cylinder (the washer heater). Complete models for the entire system may be quite complex, necessitating numerical approaches [4,9–12]. However, our goal is quite different: to calculate the temperature needed to eliminate the sharkskin, and relate that bound directly to other parameters in the problem. Therefore, a much simpler model (once which allows analytical solutions) is desirable. Results from such models have been shown to fit experimental data well [6,13].

Thus in the system at hand, we make the following simplifications:

(1) The problem is radially symmetric.
(2) We are interested in the stationary problem; that is, the steady-state flow after all transients has decayed away.
(3) The velocity is only in the $\tilde{z}$-direction at a constant V consistent with the plug-flow description (see Fig. 1). Thus, we may think of the thread flowing within the washer heater,

[1]Corresponding author.

Contributed by the Heat Transfer Division of ASME for publication in the Journal of Heat Transfer. Manuscript received August 2, 2019; final manuscript received January 23, 2020; published online March 18, 2020. Assoc. Editor: Milind A. Jog.

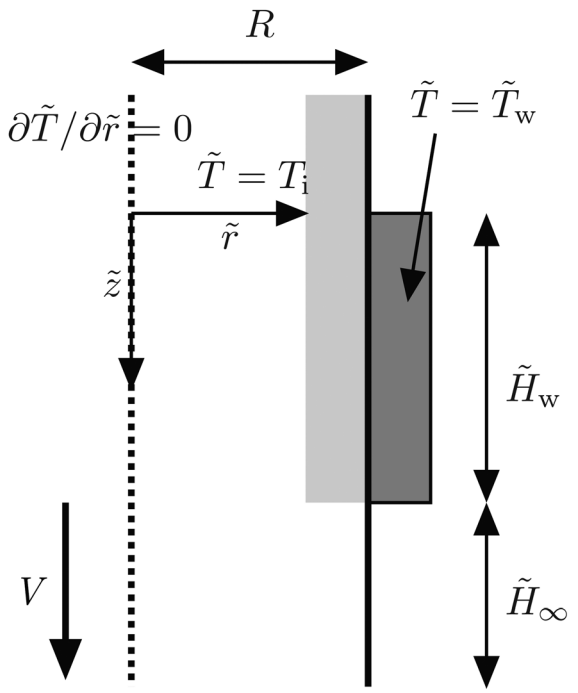

Fig. 1 Cross section of half of cylinder, dimensional coordinates. Dark shaded area is heater; light shaded area is sharkskin region. $\tilde{z} = 0$ corresponds to exit of hot end/entrance of heater.

but with a vanishingly thin air gap between the thread and the inner surface of the heater.

Assumption #3 will cause us to be too conservative with our estimates (which is the preferred direction for our errors). That is because in Poiseuille flow, the polymer near the heater would move more slowly, causing *more* relaxation of the sharkskin for a given $\tilde{H}_w$ and $\tilde{T}_w$ than our model will predict.

With these assumptions, the general dimensional equation is given by

$$V\frac{\partial\tilde{T}}{\partial\tilde{z}} = \alpha\left[\frac{1}{\tilde{r}}\frac{\partial}{\partial\tilde{r}}\left(\tilde{r}\frac{\partial\tilde{T}}{\partial\tilde{r}}\right) + \frac{\partial^2\tilde{T}}{\partial\tilde{z}^2}\right] \tag{1}$$

where $\tilde{T}$ is the temperature of the polymer and α is the thermal diffusivity. We denote $\tilde{z} = 0$ to be the upper end of the heater, which maintains the surface $\tilde{r} = R$ at a fixed temperature $\tilde{T} = \tilde{T}_w$, after which the polymer is exposed to the air for a distance $\tilde{H}_\infty$ at a temperature T_∞.

The polymer is inserted at $\tilde{z} = 0$ at an *insertion temperature* T_i. Two remarks about this temperature are appropriate:

(1) We have assumed that the initial polymer temperature is independent of $\tilde{r}$. In the hot end itself, the polymer travels through a narrowing cone after it is heated. During the traversal time, the polymer temperature should have time to equilibrate, especially since R is so small.
(2) The polymers used are either amorphous (such as ABS) or crystalline (such as PLA). We assume that T_i is above any sort of transition temperature (such as the melting temperature or glass-rubber transition) in the polymer. (See the Appendix for parameter values.)

Motivated by the discussion above, we introduce the following scalings:

$$r = \frac{\tilde{r}}{R}, \quad z = \frac{\alpha\tilde{z}}{VR^2}, \quad T(r,z) = \frac{\tilde{T}(\tilde{r},\tilde{z}) - T_\infty}{\Delta T}, \quad \Delta T = T_i - T_\infty \tag{2}$$

Note that we use the length scale that balances convection and diffusion. Substituting Eq. (2) into Eq. (1), we have the following:

$$\frac{\partial T}{\partial z} = \frac{1}{r}\frac{\partial}{\partial r}\left(r\frac{\partial T}{\partial r}\right) + \epsilon^2\frac{\partial^2 T}{\partial z^2} \tag{3a}$$

$$\epsilon = \frac{\alpha/R}{V} = \frac{\text{radial diffusion rate}}{\text{vertical velocity}} \tag{3b}$$

From the Appendix, we have that $\epsilon \ll 1$, so diffusion in the z-direction can be neglected in the washer *as long as it is thick enough*. In particular, we have the following cases:

Case 1. If $H_w = O(1)$, then z-diffusion can be neglected, and Eq. (3*a*) simplifies to

$$\frac{\partial T}{\partial z} = \frac{1}{r}\frac{\partial}{\partial r}\left(r\frac{\partial T}{\partial r}\right), \quad 0 < z < H_w \tag{4}$$

Case 2. If $H_w = O(\epsilon^a)$, $0 < a < 2$, then the washer is short enough that only the outside of the thread gets heated. (As discussed in the Appendix, H_w can be $O(\epsilon)$, so this case does apply.) Therefore, we introduce the following scalings:

$$y = \frac{z}{\epsilon^a}, \quad x = \frac{1-r}{\epsilon^{a/2}} \tag{5}$$

Substituting Eq. (5) into Eq. (3*a*), we obtain, to leading order

$$\frac{\partial T}{\partial y} = \frac{\partial^2 T}{\partial x^2}, \quad 0 < y < \frac{H_w}{\epsilon^a} = O(1) \tag{6}$$

The balance of terms is still the same: convection and x-diffusion. Hence, we expect that in this regime, we could still use the solution to Eq. (4) for small z, but with extra caution. However, the asymptotic nature of Eq. (6) makes the solution much simpler, and we will exploit this aspect of the problem when possible. This will be explored more fully in Sec. 3.

To obtain the boundary conditions, we substitute Eq. (2) into the conditions described above, which yields

$$T(1,z) = \begin{cases} T_w, & 0 < z < H_w, \\ 0, & H_w < z < H_w + H_\infty \end{cases} \tag{7a}$$

$$T(r,0) = 1 \tag{7b}$$

where we have dropped the tildes following the convention in Eq. (2). The last boundary condition required is that the centerline of the cylinder has no flux through it:

$$\frac{\partial T}{\partial r}(0,z) = 0 \tag{8}$$

The schematic in dimensionless coordinates is shown in Fig. 2.

3 The Amorphous Case

One common polymer used in 3D printing is ABS [6,7], which is amorphous. Such polymers have no phase transition, and hence the problem reduces to solving Eq. (4) subject to Eqs. (7) and (8). It is most convenient to examine the heated and exposed regions separately.

3.1 Heated Solution: Exact. In the heated region, the relevant boundary condition is given by the first line in Eq. (7*a*). Motivated by this condition, we let

$$T(r,z) = T_w - (T_w - 1)\Theta(r,z), \quad 0 \le z < H_w \tag{9}$$

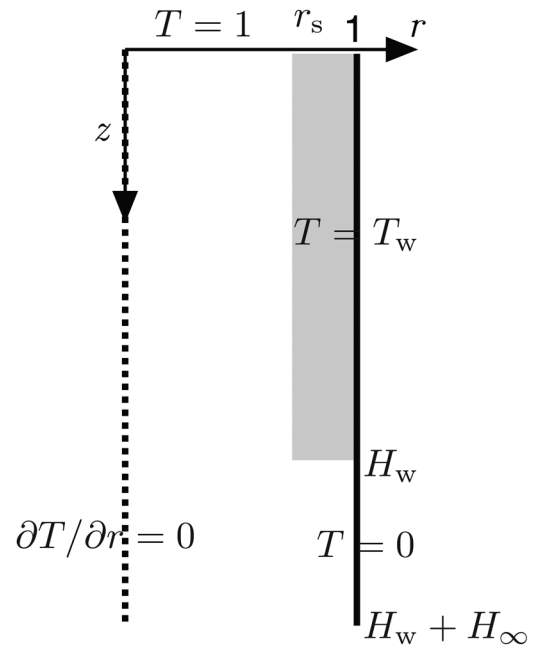

Fig. 2 Idealized dimensionless system. Light shaded area is sharkskin region.

which yields the following homogeneous problem for Θ:

$$\frac{\partial\Theta}{\partial z} = \frac{1}{r}\frac{\partial}{\partial r}\left(r\frac{\partial\Theta}{\partial r}\right), \quad \Theta(1,z) = 0, \quad \frac{\partial\Theta}{\partial r}(0,z) = 0, \quad \Theta(r,0) = 1 \tag{10}$$

It is a standard but tedious exercise in separation of variables to show that

$$\Theta_e(r,z) = \sum_{n=1}^{\infty} \frac{2}{j_{0,n}J_1(j_{0,n})} \exp\left(-j_{0,n}^2 z\right) J_0(j_{0,n}r) \tag{11}$$

where the subscript "e" stands for "exact." (The problem may also be written as a series using Laplace transform techniques, as in Ref. [14]. However, such series are typically good for large z, which is not the region in which we are interested.)

Since H_w is small, we may expect to be required to take a large number of terms in the sum in Eq. (11). However, the $j_{0,n}$ increase rapidly, so each term is exponentially smaller than the one before. That behavior dominates, *as long as z is not very near* 0. This anomaly will appear later on and be discussed further at that point.

3.2 Heated Solution: Asymptotic. Even though Eq. (11) is an exact solution which can (usually) be well approximated with just a few terms, it can be difficult to interpret given its complicated form. Therefore, (motivated by the fact that $H_w \ll 1$), we also construct the solution in the heated region for case 2 outlined in Sec. 2.

To do so, we solve Eq. (6) subject to initial and boundary conditions which are found by substituting the scalings in Eq. (5) into Eq. (7):

$$T(0,y) = T_w, \quad T(x,0) = 1 \tag{12}$$

We must also append a matching condition: to wit, at the far extent of the boundary layer, the polymer temperature must match the core temperature, which remains unchanged from its initial value

$$T(\infty,y) = 1 \tag{13}$$

For simplicity of comparison, we introduce the same substitution as in Eq. (9), except with the independent variables x and y:

$$T(x,y) = T_w - (T_w - 1)\Theta_a(x,y), \quad 0 \le z < H_w \tag{14}$$

where "a" stands for "asymptotic." Substituting Eq. (14) into our system, we have

$$\frac{\partial\Theta_a}{\partial y} = \frac{\partial^2\Theta_a}{\partial x^2}, \quad \Theta_a(0,y) = 0, \quad \Theta_a(x,0) = 1, \quad \Theta_a(\infty,y) = 1 \tag{15}$$

the solution of which is given by

$$\Theta_a(x,y) = \operatorname{erf}\left(\frac{x}{2\sqrt{y}}\right) = \operatorname{erf}\left(\frac{1-r}{2\sqrt{z}}\right) \tag{16}$$

Note that due to the self-similar structure of the solution (16), the exact width of the boundary layer is irrelevant.

3.3 Exposed Solution. To complete the analysis, we construct the solution in the thread exposed to the open air, which is the region $H_w < z < H_w + H_\infty$. In the exact case, we must solve Eq. (4) subject to the second line in Eq. (7*a*), as well as Eq. (8). Moreover, we have the following new "initial" condition, which is simply the temperature of the polymer as it exits the heater:

$$T(r,H_w) = T_w - (T_w - 1)\Theta(r,H_w) \tag{17}$$

where we have used Eq. (9). Equation (17) replaces Eq. (7*b*). The new boundary conditions are homogeneous, so $\Theta(r,z)$ already solves them. Therefore, if we let

$$T(r,z) = W(r,z) - (T_w - 1)\Theta(r,z), \quad z > H_w \tag{18}$$

in Eqs. (4), (7*a*), (8), and (17), we obtain

$$\frac{\partial W}{\partial z} = \frac{1}{r}\frac{\partial}{\partial r}\left(r\frac{\partial W}{\partial r}\right), \quad W(1,z) = 0, \quad \frac{\partial W}{\partial r}(0,z) = 0, \quad W(r,H_w) = T_w \tag{19}$$

But this is exactly the system for Θ in Eq. (10) with the following two changes:

(1) We must shift the z variable by H_w to pick up the shift in the initial condition.
(2) We must multiply by T_w to pick up the size of the initial condition.

Given these arguments, the solution to our problem is found to be

$$T(r,z) = T_w\Theta(r,z - H_w) - (T_w - 1)\Theta(r,z), \quad z > H_w \tag{20}$$

This analysis holds for both the exact and asymptotic cases; hence, we may use Eq. (20) in conjunction with either Eq. (11) or Eq. (16). The solution as constructed will not be twice continuously differentiable in z about $z = H_w$, but this will not affect the overall analysis of the problem.

4 Threshold Conditions

The first objective of the heater is to remove the sharkskin imperfections by heating the outer surface of the polymer (whether it heats the polymer below the sharkskin is largely irrelevant). Physically, we expect that if the temperature of the outer surface is above some temperature $\tilde{T}_r$ long enough for the

polymer to relax, then the imperfections will be removed. It is then natural to ask what sorts of equivalent measurable conditions will guarantee that the imperfections will vanish.

4.1 Exit Temperature. We first analyze a condition which can be easily measured experimentally. For the outer surface of the polymer to be hot enough to remove the imperfections, we posit that the sharkskin must exit the heater above some threshold temperature $\tilde{T}_*$. This condition serves as a substitute for the full condition described above, and is used by engineers. Thus, we require that

$$T(r_s, H_w) = T_*, \quad \tilde{T}_r < \tilde{T}_* < \tilde{T}_w \tag{21}$$

where r_s denotes the inner boundary of the sharkskin layer (the "s" denotes "sharkskin"; see Fig. 2). Since the temperature increases with radius, this is a sufficient guarantee.

Substituting Eq. (9) into Eq. (21) and rewriting the result in dimensional variables, we have the following:

$$\tilde{T}_w = T_\infty + \frac{\Delta T[T_* - \Theta(r_s, H_w)]}{1 - \Theta(r_s, \tilde{H}_w)} \tag{22}$$

Given values for r_s and T_*, Eq. (22) defines a relationship between H_w and T_w. Therefore, given a heater of a particular height, we can determine the minimum temperature required to relax the sharkskin. Alternatively, if we know the maximum operating temperature of the heater, we can determine the needed thickness.

A plot of the solution to Eq. (22) is shown in Fig. 3. For the range of allowable temperatures, the computed values of $\tilde{H}_w$ are (much) less than the length scale in Eq. (2), but are comparable to R. Hence, H_w is $O(\epsilon)$, and the asymptotic approximation (16) is valid. To confirm this, we graph the full solution (11) and the asymptotic solution (16) for experimentally realizable values. The experimental washers in the laboratory have

$$\tilde{H}_w = 1\,\text{mm} \quad \Rightarrow \quad \tilde{T}_w = 231\,^\circ\text{C} \tag{23}$$

where we have used Eq. (22). Note that Eq. (23) is consistent with Fig. 3.

We first graph our results versus r for $\tilde{z} = \tilde{H}_w$; the results are shown in Fig. 4. The solid curve shows the temperature using 15 terms in the series (11), while the dotted curve uses the asymptotic expression (16). Note the close agreement in the sharkskin region $[0.9, 1]$, though the asymptotic expression underestimates the true solution. Hence, using the asymptotic expression will be a conservative estimate, suggesting that we use a washer slightly longer than would be suggested using the true solution.

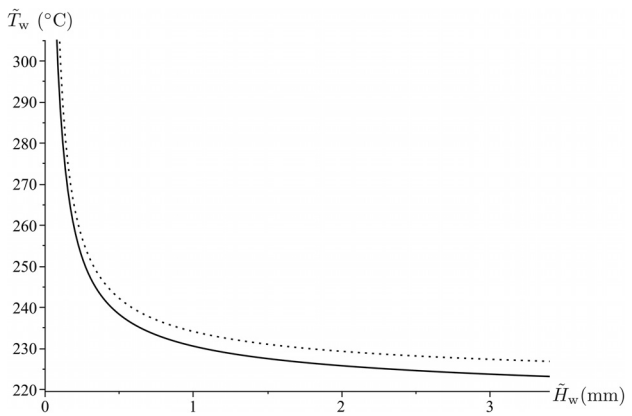

Fig. 3 Graph of $\tilde{T}_w$ required to satisfy the exit condition (22) for a given washer height $\tilde{H}_w$. Solid curve: full solution from Eq. (11). Dotted curve: asymptotic solution from Eq. (16).

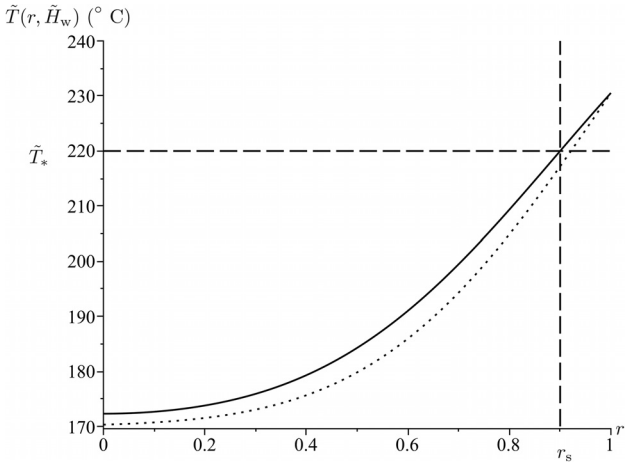

Fig. 4 Exact (solid) and asymptotic (dotted) expressions for $\tilde{T}(r, \tilde{H}_w)$ versus r for parameters in the Appendix and Eq. (23)

Though it is not in the region of interest, we note the rather surprising fact that the asymptotic solution outperforms the exact solution near $r = 0$. As alluded to in Sec. 2, for incredibly small z, the convergence of the series is very slow, while the asymptotic solution satisfies the boundary condition exactly. This effect is irrelevant to the calculation of H_w in Fig. 3, since H_w is large enough that this effect does not occur.

Due to the close agreement over the domain, we have confidence in displaying the asymptotic solution as the dotted curve in Fig. 3. As expected, the asymptotic solution is more conservative (in both temperature and thickness) than the exact solution.

The second goal of the washer heater is to keep the temperature of the outer surface hot enough not only to relax the sharkskin but also to keep it warm until bonding. Therefore, we compare the results of our reheated solution to that if there is no heater at all. (In that case, we just set $T_w = 0$ in Eq. (9), so $T(r, z) = \Theta(r, z)$ after exiting the hot end.)

The results are shown in Fig. 5. The thicker curves indicate the heated solution, which reaches $\tilde{T}_*$ at $\tilde{H}_w$, as desired. But when exposed to the open air, the temperature decreases rapidly.

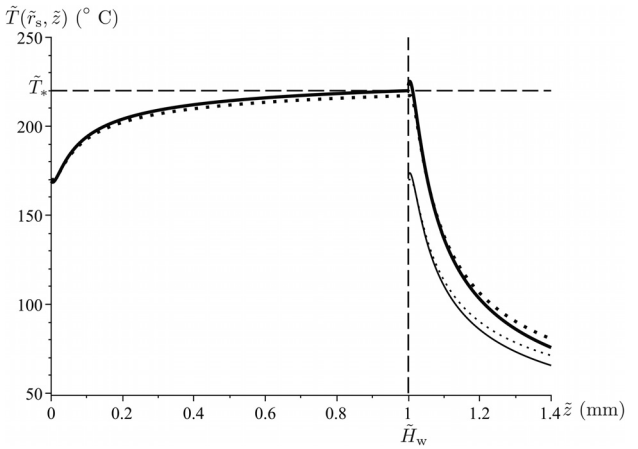

Fig. 5 Thick curves: exact (solid) and asymptotic (dotted) expressions for $\tilde{T}(r_s, \tilde{z})$ using the parameters in Eq. (23). (The exact solution uses 15 terms; the unphysical jump in the solution at the washer exit is an artifact of the slow convergence of Eq. (11) for small argument.) Thin curves: exact (solid) and asymptotic (dotted) expressions for $\tilde{T}(r_s, \tilde{z})$ if no washer heater present. ($\tilde{z}$-axis has been shifted for easy comparison with heated solution.)

The thin curves show what would happen to the thread if there were no washer present (the $\tilde{z}$-axis has been shifted for easy comparison with the thick curves). Though the thread has been heated by 50° C as it exits the heater, by the time it reaches the substrate it is only around 10° C hotter than an unheated thread. In particular,

$$\begin{aligned}\tilde{T}(\tilde{r}_s, \tilde{H}_w + \tilde{H}_\infty) &= 76\,^\circ\mathrm{C}\,(\text{heated});\\ \tilde{T}(\tilde{r}_s, \tilde{H}_w + \tilde{H}_\infty) &= 66\,^\circ\mathrm{C}\,(\text{unheated})\end{aligned} \tag{24}$$

For a given rated temperature T_w for any particular washer, one might imagine that making the washer thicker would ameliorate this problem. Unfortunately, as shown in Fig. 6, the bulk of the temperature rise occurs near the front of the washer; after that, the increase in temperature levels off. Thus making the washer several times as thick would increase the temperature only a small amount. Hence, we must conclude that the main focus of the heater must be to eliminate the sharkskin, rather than to raise the temperature at deposition significantly.

4.2 Duration. Physically, we expect that if the temperature of the sharkskin is above some temperature $\tilde{T}_r$ long enough for the polymer to relax, then the roughness will be removed. The Appendix indicates that the temperature $\tilde{T}_*$ is much higher than the glass-rubber transition temperature $\tilde{T}_g$ of the polymer. Hence, we expect that the exit temperature condition is just an experimental substitute for keeping the temperature at a lower level long enough to exceed the polymer's relaxation time.

As we have removed time from the problem, this is equivalent to stating that the temperature in the sharkskin layer remains above some relaxation temperature T_r for some interval *in* z:

$$T(r_s, z) \geq T_r, \quad z_1 \leq z \leq z_2, \quad z_2 - z_1 = z_r \tag{25}$$

where z_r denotes the (specified) dimensionless height of the relaxation region. Hence, the (dimensional) time the polymer remains over the relaxation temperature would be $\tau_r = \tilde{z}_r/V$. Equation (25) replaces Eq. (21) as the new condition on the temperature.

The position z_1 must be in the heated region, while the position z_2 must be in the exposed region. Hence, Eq. (25) can be stated in a more convenient manner as follows. First, we can use the heated condition (22), but with H_w replaced by z_1 and T_* replaced by T_r:

$$T_w = \frac{T_r - \Theta(r_s, z_1)}{1 - \Theta(r_s, z_1)} \tag{26a}$$

Then using Eq. (20), in the exposed area we must have

$$T_w = \frac{T_r - \Theta(r_s, z_1 + z_r)}{\Theta(r_s, z_1 + z_r - H_w) - \Theta(r_s, z_1 + z_r)} \tag{26b}$$

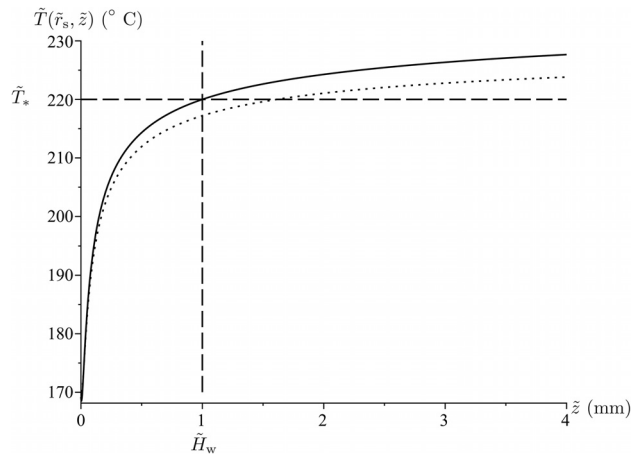

Fig. 6 Exact (solid) and asymptotic (dotted) expressions for $\tilde{T}(r_s, \tilde{z})$ for parameters in the Appendix and Eq. (23)

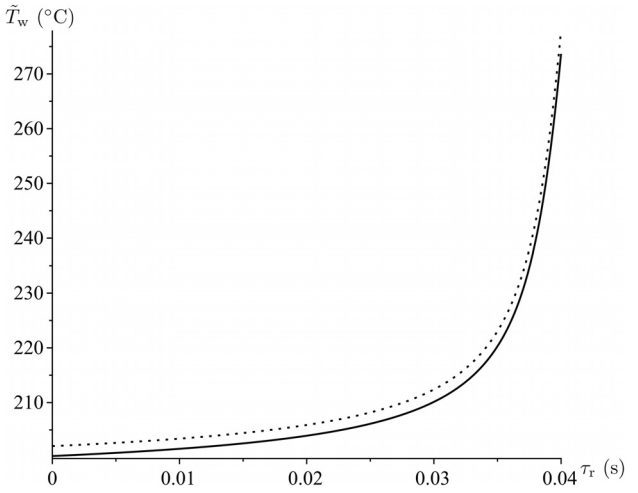

Fig. 7 Graph of $\tilde{T}_w$ required to satisfy the duration conditions (26) for a given relaxation time τ_r. Solid curve: full solution from Eq. (11). Dotted curve: asymptotic solution from Eq. (16).

where we have used Eq. (25). The system (26) will then be solved for the unknowns T_w and z_1.

For these calculations, we must assume a temperature T_r. One plausible possibility would be the glass-rubber transition temperature. However, given the parameters in the Appendix, we see from Fig. 5 that the temperature in the polymer remains above the glass/rubber transition temperature even in the case when no washer heater is present. Therefore, for simplicity, we assume

$$\tilde{T}_r = \frac{T_i + \tilde{T}_*}{2} \quad \Rightarrow \quad T_r = \frac{1 + T_*}{2} \tag{27}$$

where we have used Eq. (2)

For the possible *lengths* $\tilde{z}_r$, a reasonable upper bound is $\tilde{H}_w$. Since the thread cools very quickly once it exits the washer, most of the interval must be in the heated phase. Then translating to *time*, we have $0 \leq \tau_r \leq \tilde{H}_w/V = 0.04$ s, where we have used the parameters in the Appendix.

The results are shown in Fig. 7. As in Sec. 4.1, the asymptotic solution produces an overestimate of the temperature needed. As expected, the longer the time desired above the relaxation temperature, the higher the washer temperature must be. For small τ, the slope of the curve is small, since the desired temperature does not need to be reached until the thread is a fair distance into the cylinder. However, as τ reaches its maximum, the thread must be over the relaxation temperature for nearly all the length of the washer. Hence, the thread must be heated nearly instantaneously, which takes a much greater temperature in the washer.

This phenomenon is demonstrated more clearly in Fig. 8, which shows the temperature profiles with distance for three equally spaced values of $\tilde{T}_w$. Due to the underlying structure of the profiles, increasing the temperature 25 °C from 206 °C to 231 °C causes a much greater increase in the length of the relaxation region than raising the temperature an additional 25 °C to 256 °C. As expected, the vast majority of the relaxation region occurs in the heated region due to the rapid cooling once the thread exits the washer.

5 Crystalline Case

Another common polymer used in 3D printing is PLA [6,7], which is a crystalline polymer. The parameters in the Appendix indicate that a PLA thread will be above its melting temperature for the entire heated region—it will become crystalline only after cooling in the air (all common polymers used in 3D printing have similarly low melting temperatures). Hence, at least for the exit temperature condition, crystallization will be irrelevant.

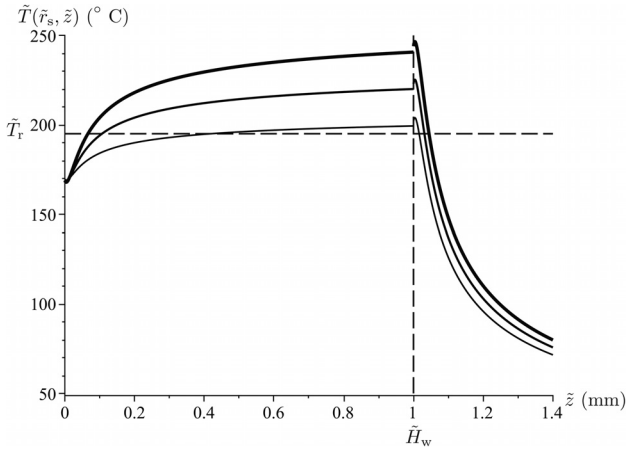

Fig. 8 Exact expressions for $\tilde{T}(r_s, \tilde{z})$. In increasing order of thickness: $\tilde{T}_w = 206\,^\circ$C, 231 °C (as in Sec. 3), and 256 °C. (The exact solution uses 15 terms; the unphysical jump in the solution at the washer exit is an artifact of the slow convergence of Eq. (11) for small argument.)

As the duration condition incorporates both the heated and unheated sections, crystallization can matter. Nevertheless, since the thread cools so quickly, we expect such effects to be small. To study this phenomenon, we analyze the Stefan problem in the exposed region.

5.1 Governing Equations. A polymer like PLA has both crystalline (subscript "c") and melted (pliant, subscript "p") states. Hence, there is a crystallization front $r = s(z)$ separating them:

$$T_c(s(z), z) = T_p(s(z), z) = T_m \tag{28}$$

where T_m is the melting temperature. The exposed surface is cooler than the crystallization temperature, so the Stefan problem begins immediately at $z = H_w$; thus $s(H_w) = 1$. The geometry is illustrated in Fig. 9. The temperature is T_c in the crystalline gray region $s < r < 1$ in the figure, while the temperature is T_p in the pliant white region $0 < r < s$.

The formulation of the Stefan condition is not straightforward due to the convection in the system. However, by switching to a moving reference frame, one may derive the proper Stefan condition [8]

$$\mathrm{St}\left[\frac{\partial T}{\partial r}\right]_s = \frac{ds}{dz}, \quad \mathrm{St} = \frac{\Delta T c_p}{c_L} \tag{29}$$

where c_p is the specific heat, c_L is the latent heat of crystallization, and $[\cdot]_s$ denotes the jump across the front. Here, St is the Stefan number. (The amorphous system is just a special case, since then $c_L = 0$, $\mathrm{St} = \infty$, and the condition is that the fluxes must match across any boundary.)

Summarizing our system, in the pliant region, we have

$$\frac{\partial T_p}{\partial z} = \frac{1}{r}\frac{\partial}{\partial r}\left(r\frac{\partial T_p}{\partial r}\right), \quad 0 < r < s(z); \quad \frac{\partial T_p}{\partial r}(0, z) = 0 \tag{30a}$$

For the initial condition for this problem, we use the temperature field at the exit

$$T_p(r, H_w) = T_w - (T_w - 1)\Theta(r, H_w) \tag{30b}$$

The equations in the crystalline region become

$$\frac{\partial T_c}{\partial z} = \frac{1}{r}\frac{\partial}{\partial r}\left(r\frac{\partial T_c}{\partial r}\right), \quad s(z) < r < 1; \quad T_c(1, z) = 0 \tag{31}$$

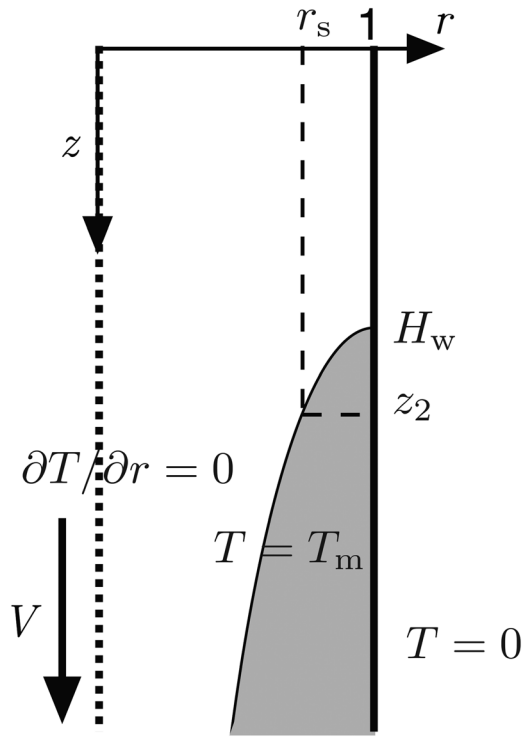

Fig. 9 Two-phase polymer system. Shaded area has crystallized.

At the front $r = s(z)$, we have the following conditions:

$$T_c(s(z), z) = T_p(s(z), z) = 0, \quad s(H_w) = 1 \tag{32a}$$

$$\frac{\partial T_c}{\partial r}(s(z), z) - \frac{\partial T_p}{\partial r}(s(z), z) = \frac{1}{\mathrm{St}}\frac{ds}{dz} \tag{32b}$$

Our system reduces to just the standard one-dimensional two-phase Stefan problem in polar coordinates with z replacing t (see also Ref. [15]).

5.2 The Quasi-Stationary Approximation. The system as posed has no analytic solution, which is the most desirable kind due to the ability to discern parameter dependence easily. To make the problem tractable, we employ the *quasi-stationary approximation*. In particular, we neglect the left-hand side of the partial differential equations (PDEs) in Eqs. (30*a*) and (31). This corresponds to taking $V \to 0$ in the dimensional equation. However, by neglecting the evolution term, we will overestimate the speed of $s(z)$ [16].

When we take the left-hand side of the PDE in Eq. (30*a*) equal to zero, the resulting equation is a second-order ordinary diffferential equation. But there are three boundary conditions to solve in Eqs. (30*b*) and (32*a*). Since, we wish to solve the problem for all time, we ignore the initial condition in Eq. (30*b*) to obtain the following solution in the pliant region:

$$T_p(r, z) \equiv T_m, \quad r < s(z) \tag{33}$$

To satisfy the initial condition, we would have to insert a thin initial layer near $z = H_w$. In this region (where the full differential equation in Eq. (30*b*) would hold), there is rapid diffusion from the initial condition to Eq. (33). (This can be thought of as an exaggerated example of the rapid cooling in the unheated region.) This effect, which is the direct result of ignoring the evolution term, will tend to overestimate the speed of $s(z)$, since it omits the

time needed to raise the polymer to the melting temperature. This will then produce a conservative estimate of the heater temperature needed, since it overstates the crystallization process.

Taking the left-hand side of the PDE in Eq. (31) equal to zero and satisfying the conditions in Eqs. (31) and (32*a*), we have

$$T_c(r,z) = \frac{T_m \log r}{\log s}, \quad s(z) < r < 1 \tag{34}$$

Depending on the experimental conditions, it may be possible for the front to hit the centerline at some $z_0 < H_w + H_\infty$:

$$s(z_0) = 0 \tag{35}$$

In that case, the steady-state operator must also satisfy the no-flux condition in Eq. (30*a*), so we have the following:

$$T_c(r,z) = 0, \quad z > z_0 \tag{36}$$

To find $s(z)$, we first substitute Eq. (33) into Eq. (32*b*), which yields

$$\frac{\partial T_c}{\partial r}(s(z),z) = \frac{1}{\mathrm{St}}\frac{ds}{dz}$$

With T_c given by Eq. (33), the problem essentially reduces to a one-phase Stefan problem. Substituting Eq. (34) into the above, we obtain

$$\frac{T_m}{s\log s} = \frac{1}{\mathrm{St}}\frac{ds}{dz}$$

Note that this equation makes sense only if $\mathrm{St} \neq \infty$; that is, only in the melting context.

Continuing to simplify, we have the following:

$$\frac{du}{dz} = \frac{4T_m}{\log u}\mathrm{St}, \quad u = s^2 \tag{37a}$$

$$4T_m\mathrm{St}(z - H_w) - 1 = u(\log u - 1) \tag{37b}$$

where in the last line we have used the initial condition in Eq. (32*a*) to determine that $u(H_w) = 1$. The solution for u can be written in terms of Lambert W-functions, but it is not illuminating.

Note from Eq. (37*b*) that the melting front hits the center of the cylinder when

$$4T_m\mathrm{St}(z_0 - H_w) - 1 = 0 \quad \Rightarrow \quad z_0 = H_w + \frac{1}{4\mathrm{St}T_m} \tag{38}$$

which matches with [16] in the case where $T_m = 1$. Hence, if $\mathrm{Pe} < 4\mathrm{St}T_m$, the entire polymer crystallizes before it is applied to the substrate. Note that z_1 depends on the quantity $\mathrm{St}T_m$, which is independent of ΔT (and hence T_∞). This makes sense since with the one-phase approximation, we are essentially assuming that the polymer leaves the washer at temperature T_m.

5.3 Duration Condition. As discussed above, crystalline polymers will be in the melt phase upon exiting the washer since $T_m < T_i$. Hence, the exit condition can be applied to both anomalous and crystalline polymers using the same model. However, the duration condition can encompass both the crystalline and melt phases.

In this case, we choose $T_r = T_m$, so $z_1 = 0$ (since $T_m < T_i$). Moreover, since $T(s(z),z) = T_m$, z_2 is given by the distance at which the crystallizing front $s(z)$ reaches r_s (see Fig. 9). Rewriting Eq. (37*b*) with this in mind, we have

$$z_r = H_w + \frac{1 + r_s^2(2\log r_s - 1)}{4T_m\mathrm{St}} \tag{39}$$

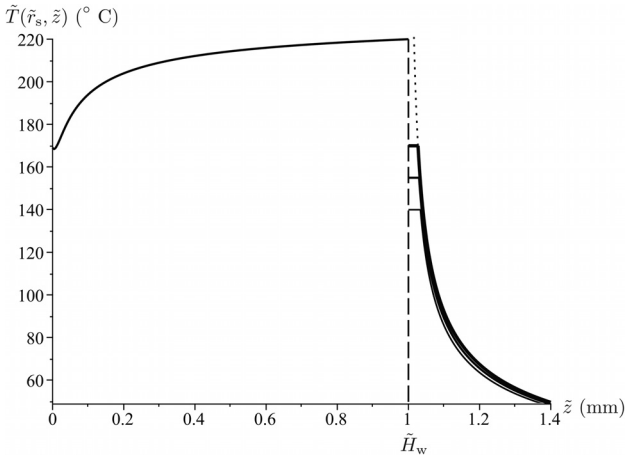

Fig. 10 Solid curves: exact expressions for $\tilde{T}(r_s,\tilde{z})$ using Eqs. (9), (33), and (34). In increasing order of thickness: $\tilde{T}_m = 140\,^\circ$C, 155 °C (actual value), and 170 °C ($\tilde{T}_i$). The quasi-stationary approximation forces the temperature to be $\tilde{T}_m$ at the exit, leading to an unphysical discontinuity there. Dotted curve: extrapolation of temperature in crystallized region to illustrate the form of the true temperature profile.

where we have used the fact that $z_1 = 0$. Unfortunately, the right-hand side is strictly determined by the material parameters and hence independent of T_w. This is because the quasi-stationary approximation implies that the temperature of the pliant core of the polymer is fixed at T_m immediately upon entering the air (see Eq. (33)). Note this is true *regardless* of the temperature at which the polymer exits the washer (which is controlled by T_w).

We present this behavior in Fig. 10, which illustrates the temperature profiles at $\tilde{r}_s$ for different $\tilde{T}_m$. The temperature drops discontinuously at $\tilde{z} = \tilde{H}_w$ to $\tilde{T}_m$ due to the quasi-stationary approximation. It then remains at $\tilde{T}_m$ until the crystallizing front reaches $\tilde{r}_s$, at which point the temperature begins to decay.

Hence, the quasi-stationary approximation will underestimate τ_r, since it really takes some time for the thread temperature to decrease to $\tilde{T}_m$. However, we do not expect the discrepancy to be that large. To see why, examine the dotted curve in Fig. 10, which extrapolates the temperature in the crystallized region (at far right) to the left until it reaches the exit temperature at only a slight distance from H_w.

Motivated by the conclusions in Ref. [8], we compare the effect of introducing the crystalline behavior at all. In particular, given that the bulk of the relaxation interval occurs in the heater, how appreciable are the effects of considering crystallization in the cooling region?

To answer this, we fix T_w and choose $T_m < T_i$. We then compare the values of τ_r using the crystalline model versus using the amorphous model with $T_r = T_m$. In particular, in this case, $z_1 = 0$, which we may substitute into Eq. (26*b*) to obtain

$$T_w = \frac{T_m - \Theta(r_s,z_r)}{\Theta(r_s,z_r - H_w) - \Theta(r_s,z_r)} \tag{40}$$

for the amorphous case.

The results are shown in Fig. 11. Since $T_m < T_i$, the polymer is above the relaxation temperature throughout the washer. Hence, $z_r > 1$, or equivalently $\tau_r > 0.04$ s. As expected, the crystalline model produces a smaller estimate of τ_r due to its unrealistic treatment of the initial drop once the polymer cools. However, this assumption does not overstate the time too much, as shown in Fig. 11. The difference is quite small (less than 7.5 ms).

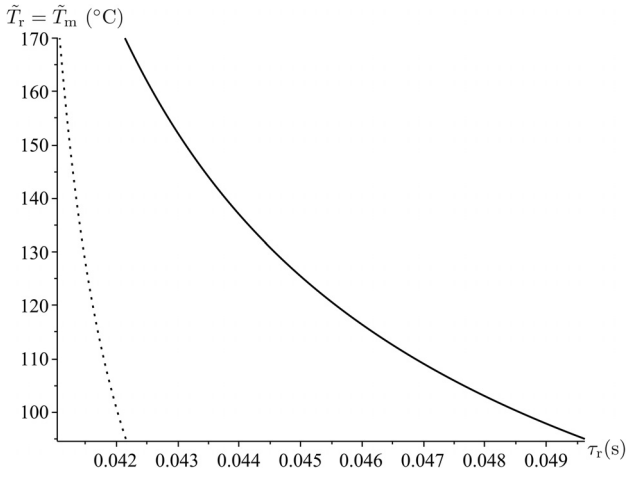

Fig. 11 Graph of the relaxation/melting temperature achieved for a given τ_r given the parameters in the Appendix. Solid curve: anomalous solution from Eq. (40). Dotted curve: crystalline solution from Eq. (39).

6 Conclusions and Further Research

It is desirable to perform additive manufacturing at the highest rate possible. However, at such high rates, the polymer feedstock does not has time to relax the stresses caused by the transition from no-slip to plug flow at the exit of the hot end. These residual stresses cause surface roughness called sharkskin, which can reduce the effectiveness of binding the polymer to the underlying substrate.

One promising approach to eliminate this problem is to reheat the polymer after it exits the hot end extrusion nozzle. This allows the polymer to relax more fully before deposition. (It may be thought that such reheating would also enhance bonding to the substrate due to the increased temperature, but we showed that the polymer is so thin that it cools very rapidly in the open air, no matter its initial temperature; see Fig. 5.)

In this paper, we investigated appropriate conditions for the design of such a postextrusion heater. After making several physically realistic simplifying assumptions, we modeled the system by the heat equation in cylindrical coordinates. The system must be solved in two regions: within the postextrusion heater where the polymer is heated, and in the open air where the polymer cools before deposition.

In the case of amorphous polymers like ABS, the resulting problem can be solved by separation of variables, which provides an exact answer which is difficult to interpret. Happily, the stresses can be relaxed even when the heater is very thin. Such a regime yields an asymptotic solution which is more easily understood.

Once the solution has been established, the more subtle point is to determine what type of conditions needs to be placed on the solution to establish a desirable experimental outcome. In particular, what must be true about the temperature in the polymer to guarantee that the sharkskin will be eliminated?

We examined two possibilities. It has been observed experimentally that the sharkskin will relax once the polymer has reached a certain temperature. For feasibility reasons, such experiments measure the temperature of the polymer at the point right after the polymer exits the postextrusion heater. Hence, we established a condition based upon this temperature.

Using this condition, we were able to produce a curve (Fig. 3) that showed (for a heater of a given thickness) the required temperature of the heater to raise the polymer temperature to the desired value. As expected, the required temperature decays rapidly with thickness. Moreover, the easily computed asymptotic solution provides conservative results, and hence can be used without concern about violating the design requirements. Fortunately, we found that the required postextrusion heater design is realizable with current technology.

In reality, the polymer will relax once the sharkskin region is heated over a certain temperature for a long enough period of time. This more realistic condition is naturally more difficult to measure, especially, since most of the time period occurs when the polymer is being heated. Given a range of relaxation times characteristic of polymers used in 3D printing, we presented results on heater temperatures which are consistent with both experimental results and the previous, simpler condition. Thus, we may feel confident that the substitute condition on the exit temperature provides useful results in the systems we wish to analyze.

Certain polymers used in the 3D printing process, such as PLA, are crystalline at low temperatures. In that case, the problem of the cooling thread becomes a Stefan problem. In order to achieve analytical solutions which we can easily interpret for parameter dependence, we used the quasi-stationary approximation to simplify the problem. It was demonstrated that the error in the temperature profiles from using such an approximation was negligible. Explicit solutions were constructed for the evolution of the front.

If we use the exit condition as our criterion, the Stefan problem does not enter into the analysis at all, since the heater remains over the crystallization temperature. The crystallization transition comes into play only when using the duration condition. In that case, we showed that treating a crystalline polymer using an amorphous model led to very small errors in our results, which is consistent with previous work [8]. Hence, using the simpler amorphous model for all types of 3D printing polymer feedstock will yield applicable results.

The model in this paper contains several listed simplifications and assumptions. Relaxing them and considering more complicated models is an area for fruitful further research. Clearly the quasi-stationary assumption for crystalline polymers could be relaxed, with an eye to doing so in a way that would make the model for crystalline polymers more experimentally realistic.

Nomenclature

Variables and Parameters

Units are listed in terms of length (L), time (T), and temperature (θ). If a symbol appears both with and without tildes, the symbol with tildes has units, while the one without is dimensionless. Equation numbers where a variable is first defined is listed, if appropriate.

a = exponent related to width of boundary layer, Eq. (5)
c_L = latent heat of melting, units L^2/T^2, Eq. (29)
c_p = heat capacity of polymer, units $L^2/(T^2\theta)$, Eq. (29)
H = height measurement, units L
R = radius of cylinder, units L
$\tilde{r}$ = radial coordinate, units L, Eq. (1)
$s(z)$ = crystallization front, units L, Eq. (28)
St = Stefan number, Eq. (29)
$\tilde{T}$ = temperature, units θ, Eq. (1)
$u(z)$ = $[s(z)]^2$, Eq. (37*a*)
V = velocity in $\tilde{z}$ -direction, units L/T, Eq. (1)
$W(r, z)$ = heat function used in transformation, Eq. (18)
x = scaled radial variable, Eq. (5)
y = scaled longitudinal variable, Eq. (5)
$\tilde{z}$ = distance along the channel, units L, Eq. (1)
α = thermal diffusivity, units L^2/T, Eq. (1)
ΔT = differential between initial and room temperature, units θ, Eq. (2)
ϵ = ratio of diffusive to convective effects, Eq. (3*b*)
Θ = heat function used in transformation, Eq. (9)
τ_r = time in relaxation state, units T

Other Notations

a = as a subscript on Θ, used to indicate an asymptotic solution, Eq. (14)

c = as a subscript on T, used to indicate the crystalline state, Eq. (28)
e = as a subscript on Θ, used to indicate an exact solution, Eq. (11)
i = as a subscript on T, used to indicate the initial temperature
m = as a subscript on T, used to indicate the melting temperature, Eq. (28)
p = as a subscript on T, used to indicate the pliant state, Eq. (28)
r = as a subscript, used to indicate relaxation
s = as a subscript on r, used to indicate the sharkskin, Eq. (21)
w = as a subscript, used to indicate the washer heater
$*$ = as a subscript on T, used to indicate the desired condition, Eq. (21)
∞ = as a subscript, used to indicate the exposed air

Appendix

In Table 1 we list the parameters for the general experimental setup, which come directly from measurements in the lab. As hypothesized, the aspect ratio of the cylinder is small: $O(10^{-2})$. Note that $\tilde{H}_\infty$ is comparable to R, so $H_\infty = O(\epsilon)$. Examining the range of $\tilde{H}_w$ in Fig. 3, we have that

$$0 \le \tilde{H}_w \le 3.5\,\text{mm} \quad \Rightarrow \quad 0 \le H_w \le 0.224$$

and hence we see that H_w can be $O(\epsilon)$, as required for our asymptotic analysis to hold. In particular, the value of $\tilde{H}_w = 1$ mm given in Eq. (23) corresponds to $H_w = 4\epsilon$.

In Table 2, we list the parameters for ABS. In the left column are experimental parameters; the values of the calculated parameters are listed at right. As expected, T_i is far above the glass-rubber transition temperature $\tilde{T}_g$.

In Table 3, we list the material parameters for PLA. As expected, T_i is far above both the glass-rubber transition temperature $\tilde{T}_g$ and the crystallization temperature $\tilde{T}_m$. To estimate the relaxation time of the PLA, we use the approximation that

$$\tau_r = \frac{\sum_i \lambda_i G_i}{\sum_i G_i} \tag{A1}$$

where the values of the parameters on the right-hand side are given in Ref. [6]. Note that the value in Table 3 compares favorably with the time scales shown in Fig. 7.

Table 1 General device parameters

Experimental		Calculated	
$\tilde{H}_\infty$ (mm)	0.4	H_∞	2.56×10^{-2}
R (mm)	0.25	r_s	0.9
$\tilde{T}_w$ (°C)	300	T_w	1.87
$\tilde{T}_*$ (°C)	220	T_*	1.33
T_∞ (°C)	20	ΔT (°C)	150
T_i (°C)	170	ϵ	0.016
V (mm/s)	25		
α (mm^2/s)	0.1		

Table 2 Parameters for ABS

	Experimental [6]	Used	Calculated	
$\tilde{T}_g$ (°C)	100			
$\tilde{T}_r$ (°C)		195	T_r	1.17

Table 3 Parameters for PLA

	Experimental [6]	[17]	Calculated	
c_L (kJ/kg)		91	St	2.80
c_p (J/(kg·K))	1700			
$\tilde{T}_g$ (°C)	59			
$\tilde{T}_m$ (°C)	155		T_m	0.9
τ_r (s)	1.23×10^{-2}			

References

[1] Gibson, I., Rosen, D. W., and Stucker, B., 2009, *Additive Manufacturing Technologies: Rapid Prototyping to Direct Digital Manufacturing*, 1st ed., Springer Publishing Company, New York.
[2] Miller, E., Lee, S. J., and Rothstein, J. P., 2006, "The Effect of Temperature Gradients on the Sharkskin Surface Instability in Polymer Extrusion Through a Slit Die," Rheol. Acta, **45**(6), pp. 943–950.
[3] Grant, M., Shore, J., Ronis, D., and Piché, L., 1997, "Theory of Melt Fracture Instabilities in the Capillary Flow of Polymer Melts," Phys. Rev. E, **55**(3), pp. 2976–2992.
[4] Wilson, I., and Rough, S., 2006, "Exploiting the Curious Characteristics of Dense Solid–Liquid Pastes," Chem. Eng. Sci., **61**(13), pp. 4147–4154.
[5] Prajapati, H., Ravoori, D., and Jain, A., 2018, "Measurement and Modeling of Filament Temperature Distribution in the Standoff Gap Between Nozzle and Bed in Polymer-Based Additive Manufacturing," Addit. Manuf., **24**, pp. 224–231.
[6] Mackay, M. E., Swain, Z. R., Banbury, C. R., Phan, D. D., and Edwards, D. A., 2017, "The Performance of the Hot End in a Plasticating 3D Printer," J. Rheol., **61**(2), pp. 229–236.
[7] Phan, D. D., Swain, Z. R., and Mackay, M. E., 2018, "Rheological and Heat Transfer Effects in Fused Filament Fabrication," J. Rheol., **62**(5), pp. 1097–1107.
[8] Edwards, D. A., Mackay, M. E., Swain, Z. R., Banbury, C. R., and Phan, D. D., 2019, "Maximal 3D Printing Extrusion Rates," IMA J. Appl. Math., **84**(5), pp. 1022–1043.
[9] Lotero, F., Couenne, F., Maschke, B., and Sbarbaro, D., 2017, "Distributed Parameter Bi-Zone Model With Moving Interface of an Extrusion Process and Experimental Validation," Math. Comput. Modell. Dyn. Syst., **23**(5), pp. 504–522.
[10] Mu, Y., Zhao, G., Wu, X., Hang, L., and Chu, H., 2015, "Continuous Modeling and Simulation of Flow-Swell-Crystallization Behaviors of Viscoelastic Polymer Melts in the Hollow Profile Extrusion Process," Appl. Math. Model., **39**(3–4), pp. 1352–1368.
[11] Sandoval Murillo, J. L., and Ganzenmueller, G. C., 2017, "A Convergence Analysis of the Affine Particle-in-Cell Method and Its Application in the Simulation of Extrusion Processes," Five International Conference on Particle-Based Methods—Fundamentals and Applications (Particles 2017), pp. 397–408.
[12] Schoinochoritis, B., Chantzis, D., and Salonitis, K., 2017, "Simulation of Metallic Powder Bed Additive Manufacturing Processes With the Finite Element Method: A Critical Review," Proc. Inst. Mech. Eng. B, **231**(1), pp. 96–117.
[13] Coasey, K., Hart, K. R., Wetzel, E., Edwards, D., and Mackay, M. E., "Nonisothermal Welding in Fused Filament Fabrication," Addit. Manuf., accepted.
[14] Carrier, G. F., and Pearson, C. E., 1988, *Partial Differential Equations: Theory and Technique*, Academic Press, New York.
[15] Hill, J. M., and Wu, Y. H., 1994, "On a Nonlinear Stefan Problem Arising in the Continuous Casting of Steel," Acta Mech., **107**(1–4), pp. 183–198.
[16] Alexiades, V., and Solomon, A. D., 1992, *Mathematical Modeling of Melting and Freezing Processes*, Taylor & Francis, Washington, DC.
[17] Pyda, M., Bopp, R., and Wunderlich, B., 2004, "Heat Capacity of Poly(Lactic Acid)," J. Chem. Thermodyn., **36**(9), pp. 731–742.